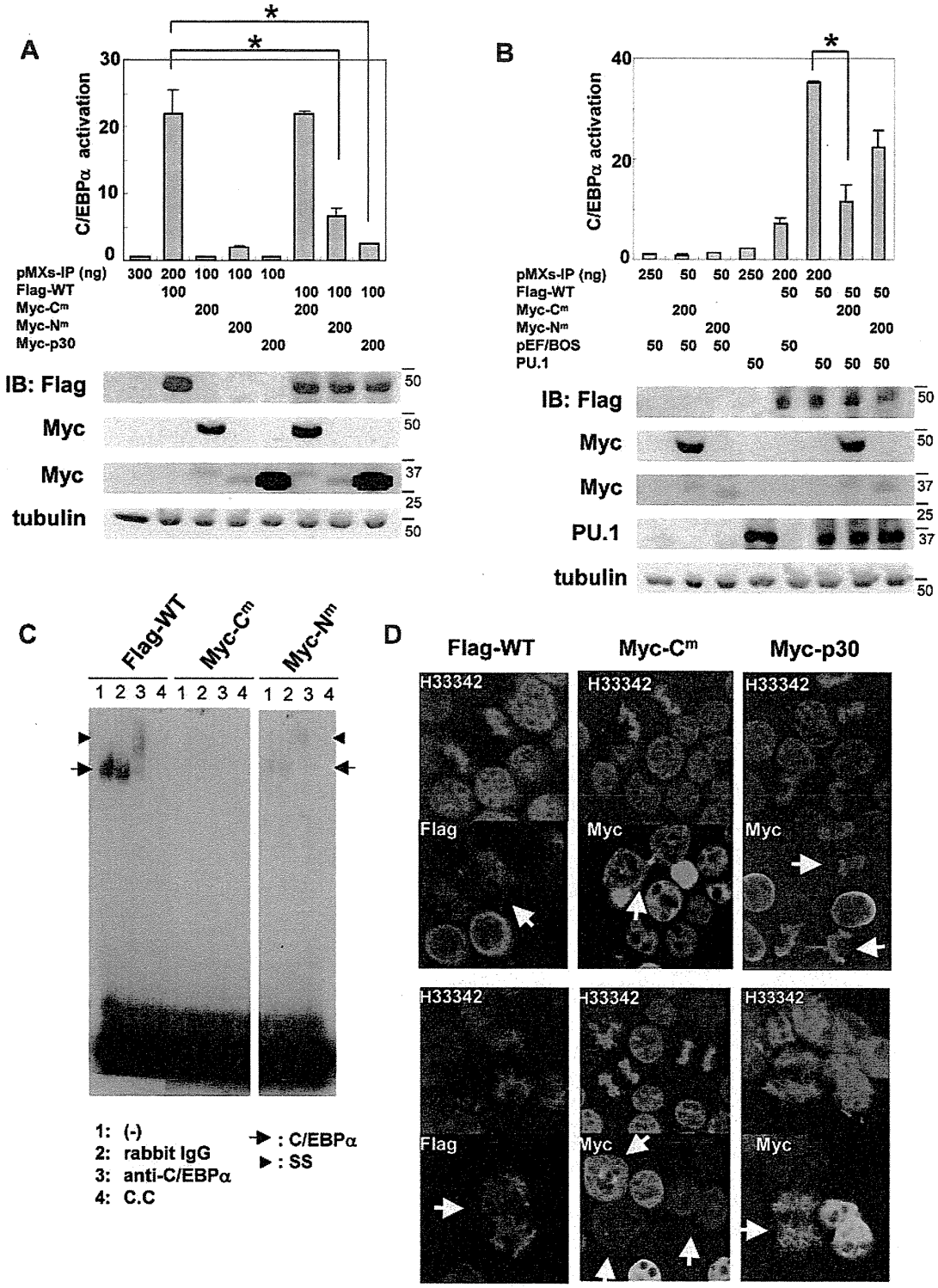

Figure 2. C/EBPα-C^m or C/EBPα-N^m inhibited the transcriptional activation of C/EBPα-WT by different mechanisms. (A-B top) 293T cells were transiently transfected with indicated amounts of expression plasmids (pMXs-Flag-tagged C/EBPα WT-IP, pMXs-Myc-tagged C/EBPα mutants-IP, pMXs-IP, pEF-BOS/PU.1, pEF-BOS) together with 100 ng of the luciferase reporter plasmid p(C/EBP)2TK. The total amount of plasmid for each transfection was adjusted by adding empty plasmids (pMXs-IP or pEF-BOS). Results represented the average values for relative luciferase activity that were normalized using the activity of EF1 vector as an internal control. All transfection groups were normalized with a Renilla luciferase vector as an internal control. All data points correspond to the mean and the standard deviation (SD). Data are representative of 3 independent experiments. Statistically significant differences are shown. *$P < .05$. (Bottom) Expression of C/EBPα-WT, C/EBPα-mutants, or PU.1 in 293T cells transiently transfected as above described. Cell lysates were subject to immunoblotting with anti-Flag Ab, anti-Myc Ab, anti-PU.1 Ab, or anti-tubulin Ab as control. The results shown are representative of 3 independent experiments. (C) DNA binding of C/EBPα-WT and mutants. Electrophoresis mobility shift assay was performed with ^{32}P-labeled oligonucleotides containing the C/EBPα binding site derived from CSF3R promoter and nuclear extracts from 293T cells transiently transfected with pMXs-Flag–tagged C/EBPα WT-IP, pMXs-Myc–tagged C/EBPα-C^m-IP, or pMXs-Myc–tagged C/EBPα-N^m-IP. Data are representative of 3 independent experiments. Lane 1: none (−); lane 2: control rabbit immunoglobulin G was added; lane 3: anti-C/EBPα Ab was added; lane 4: cold competitor (C.C) was added. Ss indicates supershifted bands. (D) 293T cells transiently transfected with pMXs-Flag–tagged C/EBPα-WT-IP, pMXs-Myc-tagged C/EBPα-C^m-IP, or pMXs-Myc–tagged C/EBPα-p30-IP were immunostained with anti-Flag Ab (red) or anti–c-Myc Ab (green) and stained with Hoechst (H33342; blue). Data are representative of 4 independent experiments (total of 15 mitotic cells were examined for each transfectant). Fluorescence images by confocal microscopy were obtained with IX70 (Olympus). Original magnification ×60.

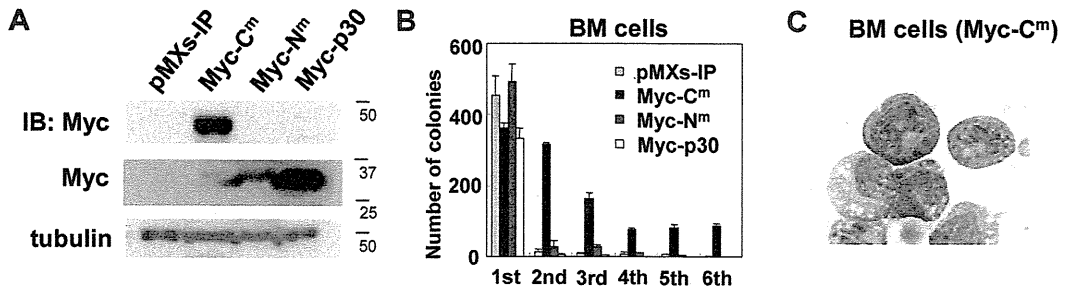

Figure 3. C/EBPα-C^m, but not C/EBPα-N^m, immortalized BM cells. (A) Expression of C/EBPα-C^m, C/EBPα-N^m, or C/EBPα-p30 in BM cells transduced with Myc-tagged C/EBPα-C^m, C/EBPα-N^m, C/EBPα-p30, or mock (pMXs-IP). Cell lysates were subject to immunoblotting with anti-Myc Ab or anti-tubulin Ab as control. The results shown are representative of 3 independent experiments. (B) Colony-forming assay from BM cells transduced with C/EBPα-C^m, C/EBPα-N^m, C/EBPα-p30, or mock (pMXs-IP). Bars represent the number of colonies obtained per 10^4 cells after each round of plating in methylcellulose supplemented with stem cell factor, thrombopoietin, IL-3, and IL-6. Data are representative of 3 independent experiments. All data points correspond to the mean and the standard deviation (SD) of 3 independent experiments. (C) Cytospin preparations of immortalized BM cells transduced with C/EBPα-C^m were stained with Giemsa. Images were obtained with a BX51 microscope and a DP12 camera (Olympus); objective lens, UplanFl (Olympus); original magnification ×100.

(Figure 3A). We also confirmed that the expression levels of p30 protein generated by C/EBPα-p30 are higher than those by C/EBPα-N^m (Figure 3A). Irrespective of different expression levels of p30, most C/EBPα-N^m- and C/EBPα-p30–transduced BM cells did not make secondary colonies after replating (Figure 3B). On the other hand, BM cells expressing C/EBPα-C^m formed colonies after 6 rounds of replating in the presence of cytokine cocktail (Figure 3B). Cytospin preparations of these cells showed blastlike morphologies (Figure 3C). In addition, C/EBPα-C^m–transduced BM cells remained immature and were immortalized in a liquid culture containing IL-3 after several rounds of the replating in semisolid cultures.

Transduction with C/EBPα-C^m into BM cells caused AML in a mouse BMT model

To test whether a single C/EBPα mutant induces hematopoietic abnormality, Ly-5.1 murine BM mononuclear cells, infected with retroviruses harboring C/EBPα-C^m, C/EBPα-N^m, or mock (pMYs-IG), were transplanted into irradiated syngenic Ly-5.2 mice. We confirmed efficient retrovirus infection: 50%-65% of BM cells transduced with C/EBPα-N^m or mock (pMYs-IG) and 35%-50% of BM cells transduced with C/EBPα-C^m were positive for GFP expression before transplantation. Mice receiving transplants of mock (pMYs-IG)–transduced cells (hereafter referred to as mice/pMYs-IG) remained healthy over the observation period (n = 8/8) (Figure 4A). Notably, most of the mice that received transplants of C/EBPα-C^m–transduced cells (hereafter referred to as mice/C^m) developed AML within 4-12 months after transplantation (n = 16/17) (Figure 4A). These morbid mice presented similar phenotypes, characterized by hepatosplenomegaly and pancytopenia (Table 2). BM and spleen were occupied with myeloblasts and myelocytes (Figure 4B). In some cases, leukemic cells displayed morphologic aberrations such as abnormal lobular and ring-shaped nucleus. GFP-positive leukemic cells expressed CD11b and Gr-1 at high levels and c-kit at intermediate to high levels (middle panel in Figure 4C). One of the mice/C^m developed T-cell lymphoma with thymoma (data not shown). We next asked if the integration of retroviruses influenced the outcomes in the BMT model. Southern blot analysis of BM cells of mice/C^m showed a single or several integrations (supplemental Figure 4), and either 1 or 2 integration sites were identified in these samples, based on the inverse PCR method (supplemental Table 1).[47] We found several common integration sites and integrations of the retroviruses in the intron of MN1 in 2 of 15 cases examined (supplemental Table 1). Considering the recent works published by Hasemann et al[48] and by ourselves,[40] retrovirus integration might in part influence the phenotypes of the recipient mice in our BMT models. For example, integration of the retrovirus vector into MN1 may enhance cell growth.[40] However, integration sites do not seem to play major roles in the experiments of this study; C/EBPα-C^m transduction induced AML with similar phenotypes in most cases after a relatively long latency in the BMT model. On the other hand, 5 of 8 mice that received transplants of C/EBPα-N^m–transduced cells (hereafter referred to as mice/N^m) remained healthy during the observation period. Three of 8 mice/N^m developed B-cell acute lymphoblastic leukemia (B-ALL) with hepatosplenomegaly with latencies of 7 to 12 months after transplantation (Figure 4A). BM was occupied with blastlike cells, and the morbid mice exhibited leukocytosis, anemia, and thrombocytopenia (Figure 4B and data not shown). GFP-positive leukemic cells expressed B220 and CD19 at high levels and c-kit at intermediate to high levels (right panel in Figure 4C). One of the mice/N^m developed AML with splenomegaly 13 months after transplantation (data not shown). The reason why C/EBPα-N^m tend to induce B-ALL is not clear. However, we must notice a point that mouse BMT models may not always mimic human diseases.[35,40] Expression of C/EBPα-C^m in spleen cells of mice/C^m with AML or p30 protein generated by C/EBPα-N^m in spleen cells of mice/N^m with B-ALL was confirmed by Western blot analysis (Figure 4D). Collectively, C/EBPα-C^m has a potential to strongly induce AML in a BMT model. Because the latency is relatively long and the leukemic cells seem to be clonal, additional events should have worked with C/EBPα-C^m in inducing leukemia. In addition, the in vivo suppressive effect of C/EBPα-C^m on the activation of endogenous C/EBPα was confirmed by the finding that G-CSF-R expression was down-regulated and c-Myc expression was up-regulated in BM samples of mice/C^m compared with mice/pMYs-IG (Figure 4E-F).

Transduction with both C/EBPα-C^m and C/EBPα-N^m induced more aggressive AML with leucocytosis

To next ask whether the combination of both C/EBPα-C^m and C/EBPα-N^m would induce AML more efficiently, we performed BMT, using murine BM mononuclear cells infected with retroviruses harboring Myc-tagged C/EBPα-C^m-IRES-GFP and Flag-tagged C/EBPα-N^m-IRES-dsRED. BM mononuclear cells expressing both mutants were recognized as GFP- and dsRED-double positive cells, 10%-22% of BM cells before the transplantation. Notably, mice that had received transplants of BM cells expressing both mutants (hereafter referred to as mice/Myc-C^m/Flag-N^m) developed AML with hepatosplenomegaly with shorter latencies

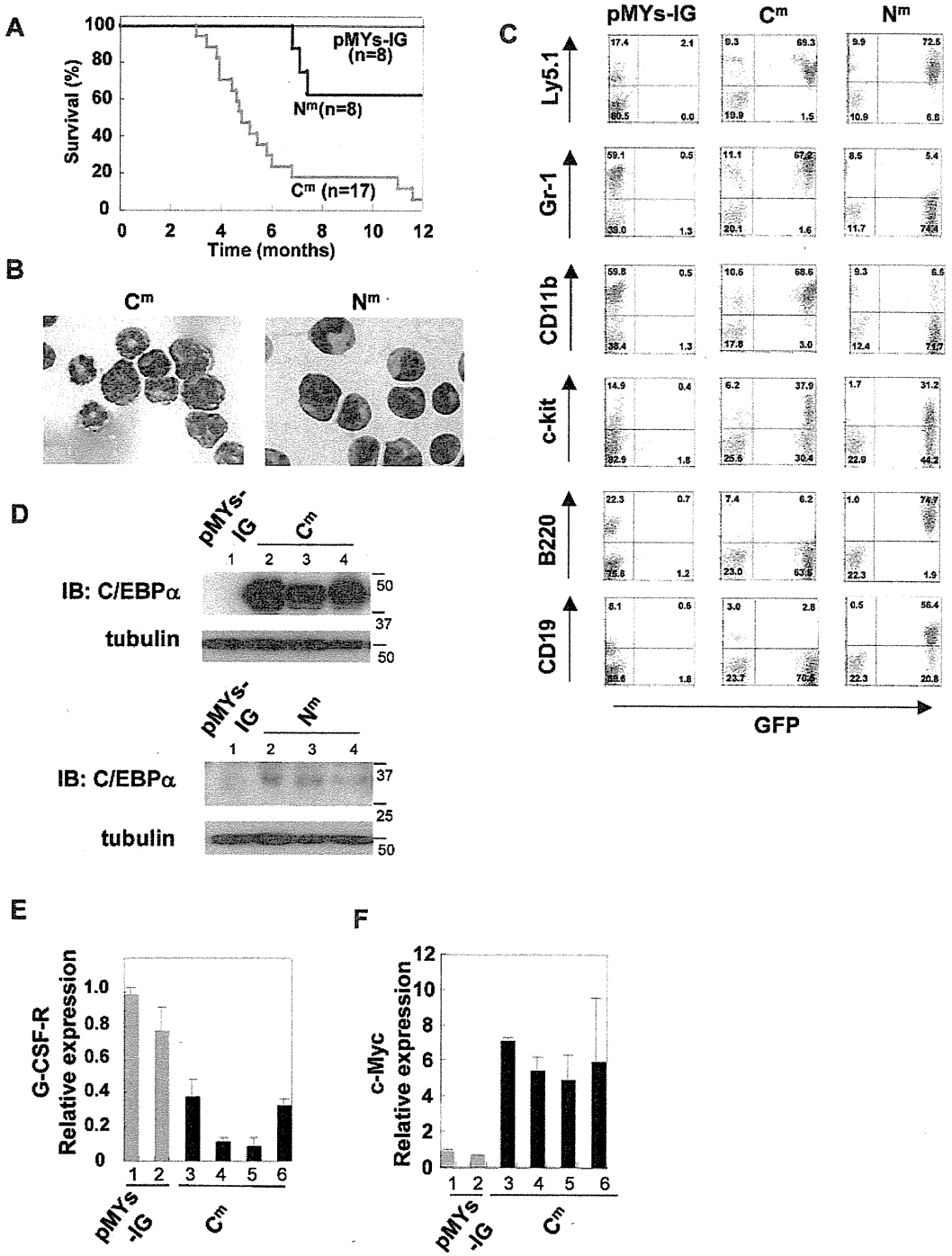

Figure 4. Transduction with C/EBPα-C^m alone induced AML in a mouse BMT model. (A) Kaplan-Meier analysis for the survival of mice that received transplants of BM cells transduced with C/EBPα-C^m-IG (C^m, n = 17), C/EBPα-N^m-IG (N^m, n = 8), or mock (pMYs-IG, n = 8). (B) Cytospin preparations of BM cells derived from mice/C/EBPα-C^m (left) or mice/N^m (right) were stained with Giemsa. A representative photograph is shown. Images were obtained with a BX51 microscope and a DP12 camera (Olympus); objective lens, UplanFl (Olympus); original magnification ×100. (C) Flow cytometric analysis of BM cells derived from mice/C/EBPα-C^m (middle), mice/C/EBPα-N^m (right), or mice/pMYs-IG (left). The dot plots show Ly5.1, Gr-1, CD11b, c-kit, B220, or CD19 labeled with phycoerythrin-conjugated monoclonal Ab versus expression of GFP. (D) Expression of C/EBPα-C^m protein and p30 protein generated by C/EBPα-N^m in spleen cells of mice/pMYs-IG (lane 1) and mice/C^m (lanes 2-4) (top) or in spleen cells of mice/pMYs-IG (lane 1) and mice/N^m (lanes 2-4) (bottom). Cell lysates were subject to immunoblotting with anti-C/EBPα (14AA) Ab or anti-tubulin Ab as control. Data are representative of 3 independent experiments. (E-F) Real-time PCR for G-CSF-R (E) or c-Myc (F) in BM cells derived from mice/C^m or mice/pMYs-IG. Expression levels were normalized by β-actin mRNA. The relative expression level of BM derived from mice/mock (lane 1) was defined as 1. All data points correspond to the mean and the standard deviation (SD) of 3 independent experiments. Lanes 1-2: mice/pMYs-IG; lanes 3-6: mice/C^m.

(3-5 months) compared with mice that had received transplants of BM cells expressing both Myc-C^m-IRES-GFP and mock (pMYs-IR, hereafter referred to as mice/Myc-C^m/pMYs-IR; Figure 5A). Of note, there was no significant difference of the phenotypes between mice/C^m and mice/Myc-C^m/pMYs-IR or between mice/N^m and mice that had received transplants of BM cells expressing both mock (pMYs-IG) and Flag-N^m-IRES-dsRED (hereafter referred to as mice/pMYs-IG/Flag-N^m; Figures 4-5 and data not shown). The percentages of the immature blast ranged from 72%-94% in mice/Myc-C^m/Flag-N^m (Table 2) compared with 62%-92% in

Table 2. Characteristics of AML caused by C/EBPα mutants

	pMYs-IG/pMYs-IR (n = 8)	Myc-C^m/pMYs-IR (n = 6)	Myc-C^m/Flag-N^m (n = 8)
WBC (/μL)	9060 ± 1648	5816 ± 3128	36 675 ± 22 956
Hb (g/dL)	16.4 ± 3.2	12.4 ± 2.2	10.7 ± 2.3
Plt (× 10^4/μL)	79.4 ± 43.1	7.2 ± 4.5	19.8 ± 13.1
BM count (× 10^7)	3.34 ± 0.73	1.69 ± 0.30	2.83 ± 0.88
Leukemic cells (%)	-	60-92	72-94
Liver weight (mg)	1433 ± 153	2071 ± 1281	2441 ± 1315
Spleen weight (mg)	113 ± 24	476 ± 220	549 ± 239

Averages and standard deviations are shown. BM cells were isolated from both tibias and femurs.

WBC indicates white blood cell; Hb, hemoglobin; and Plt, platelets.

C/EBPα-C^m–induced leukemia (Table 2 and Figure 5B). Morphologies of the leukemic blasts are more immature in mice/Myc-C^m/Flag-N^m than mice/Myc-C^m/pMYs-IR (Figure 5B), consistent with the lower expression of Gr-1 in the former (Figure 5C and data not shown). Flow cytometric analysis delineated that most leukemic cells of mice/Myc-C^m/Flag-N^m expressed both GFP and dsRED (Figure 5C) and invariable markers: CD11b-inntermediate and Gr-1, B-220, c-kit-low (Figure 5C). Expression of both C/EBPα-C^m protein and p30 protein generated by C/EBPα-N^m in leukemic cells of mice/Myc-C^m/Flag-N^m was confirmed by Western blot analysis (Figure 5D). Expression levels of p30 protein generated by C/EBPα-N^m were not correlated with the disease latency in mice/Myc-C^m/Flag-N^m (Figure 5A,D). The morbid mice/Myc-C^m/Flag-N^m suffered from anemia and thrombocytopenia-like mice/Myc-C^m/pMYs-IR; however, it was of note that unlike mice/Myc-C^m/pMYs-IR, most mice/Myc-C^m/Flag-N^m exhibited marked leukocytosis (Figure 5E-F and Table 2). These results suggested that C/EBPα-N^m either confers a proliferative advantage on immature myeloid cells or collaborates with C/EBPα-C^m in blocking differentiation of myeloid cells in vivo. It is of note that this collaborative effect was induced by relatively low levels of p30 protein generated by C/EBPα-N^m.

C/EBPα-C^m, but not C/EBPα-N^m, collaborated with Flt3-ITD in inducing AML in a BMT model

Because C/EBPα-C^m possessed the potential to strongly suppress myeloid differentiation, this mutation could be categorized into class II mutations. We speculated that AML would be efficiently induced by combining C/EBPα-C^m with class I gene alterations. To test this, murine BM mononuclear cells, transduced with both Flt3-ITD and either C/EBPα-C^m or C/EBPα-N^m, were transplanted into the recipient mice. BM mononuclear cells expressing both mutants were recognized as GFP- and dsRED-double positive cells, 10%-20% of BM cells before the transplantation. As reported previously,[49] mice receiving transplants of BM cells expressing both Flt3-ITD-IRES-GFP and mock (pMYs-IR) (mice/FLT/pMYs-IR) developed myeloproliferative neoplasm (MPN) within 1.5-3 months after transplantation (Figure 6A). BM and spleen were occupied with increased numbers of mature myeloid cells expressing CD11b at high levels and Gr-1 at intermediate to high levels (Figure 6B-C). Intriguingly, mice transplanted with BM cells expressing both Flt3-ITD-IRES-GFP and C/EBPα-C^m-IRES-dsRED (mice/FLT/C^m) developed aggressive leukemia within 2-3 weeks after transplantation (Figure 6A). Histologic examination of mice/FLT/C^m showed that BM was occupied with the 2 populations: large and small blastlike cells (Figure 6B). However, flow cytometric analysis demonstrated that both populations, double positive for GFP and dsRED, similarly expressed B220, CD19, Gr-1, and CD11b and could not be differentiated (Figure 6C and data not shown). Thus, mice/FLT/C^m invariably developed biphenotypic leukemia. Western blot analysis demonstrated that both Flt3-ITD and C/EBPα-C^m proteins were expressed in spleen cells of mice/FLT/C^m (Figure 6D). On the other hand, mice that received transplants of BM cells expressing both Flt3-ITD-IRES-GFP and C/EBPα-N^m-IRES-dsRED (mice/FLT/N^m) developed MPN with latencies comparable with those of MPN developed by mice/FLT/pMYs-IR, although some lymphoid blast cells were observed in 2 mice/FLT/N^m (Figure 6A and data not shown). Thus, C/EBPα-N^m did not significantly collaborate with Flt3-ITD in leukemogenesis in the present BMT model. Finally, leukemic cells derived from mice/FLT/C^m proliferated independently of IL-3 in the culture, while those from mice/C^m still required IL-3 for their growth. Leukemic cells derived from mice/FLT or mice/FLT/N^m did not survive even in the presence of IL-3. Moreover, we found stronger activation of STAT5, STAT3, AKT, and ERK in leukemic cell lines derived from mice/C^m/FLT compared with those from mice/C^m (Figure 6E). These results indicated that Flt3-ITD conferred additional proliferative potentials as a class I mutation on the cells expressing C/EBPα-C^m alone, thereby inducing aggressive leukemia.

Discussion

The present results on *CEBPA* mutations of AML patients confirmed previous reports[20-28]; *CEBPA* mutations are found in 5%-14% of de novo AML, and most of them harbor 2 distinct mutations on different alleles and have good prognosis. In addition, our results suggested that mutations of *CEBPA* are found only in one allele in most cases of therapy-related AML or MDS, and AML progressed from MDS harboring CEBPA mutations (8/71 and 7/224). While we did not find additional mutations in other genes in de novo AML patients with double CEBPA mutations, we detected 3 additional mutations in 15 patients with therapy-related AML or MDS and MDS/AML. These results indicate that a *CEBPA* mutation collaborates with either a different type of CEBPA mutations or mutations in different genes in inducing leukemia.

Analysis of CEBPA mutations in in vitro assays provided novel insights concerning the role of CEBPά in blood cells. C/EBPα-N^m and p30, but not C/EBPα-C^m, suppressed transcriptional activation of C/EBPα-WT in a luciferase assay using 293T cells (Figure 2A) as reported previously.[20] Curiously, expression of G-CSF-R, a major target of C/EBPα, was profoundly suppressed by C/EBPα-C^m but not by C/EBPα-N^m in 32Dcl3 cells (Figure 1F). C/EBPα-C^m suppressed G-CSF–induced granulocytic differentiation of 32Dcl3 cells more efficiently than C/EBPα-N^m (Figure 1D-E). It is possible that insufficient suppression of G-CSF–induced differentiation of 32Dcl3 cells by C/EBPα-N^m despite its inhibitory activity on transcriptional activation of C/EBPα-WT in 293T cells may be because of the low expression of C/EBPα-N^m in 32Dcl3 cells (Figure 1B). In fact, C/EBPα-p30 moderately suppressed the expression of G-CSF-R and inhibited G-CSF–induced differentiation of 32Dcl3 cells (Figure 1D-F). However, this does not explain why C/EBPα-C^m efficiently blocks the differentiation of 32Dcl3 cells despite its inability to suppress C/EBPα activation in the luciferase assay. Therefore, we speculated that C/EBPα mutants behave differently in epithelial 293T cells and hematopoietic 32Dcl3 cells and tested whether hemotopoietic cell–specific transcription factors play some role in 32Dcl3 cells. Because it was

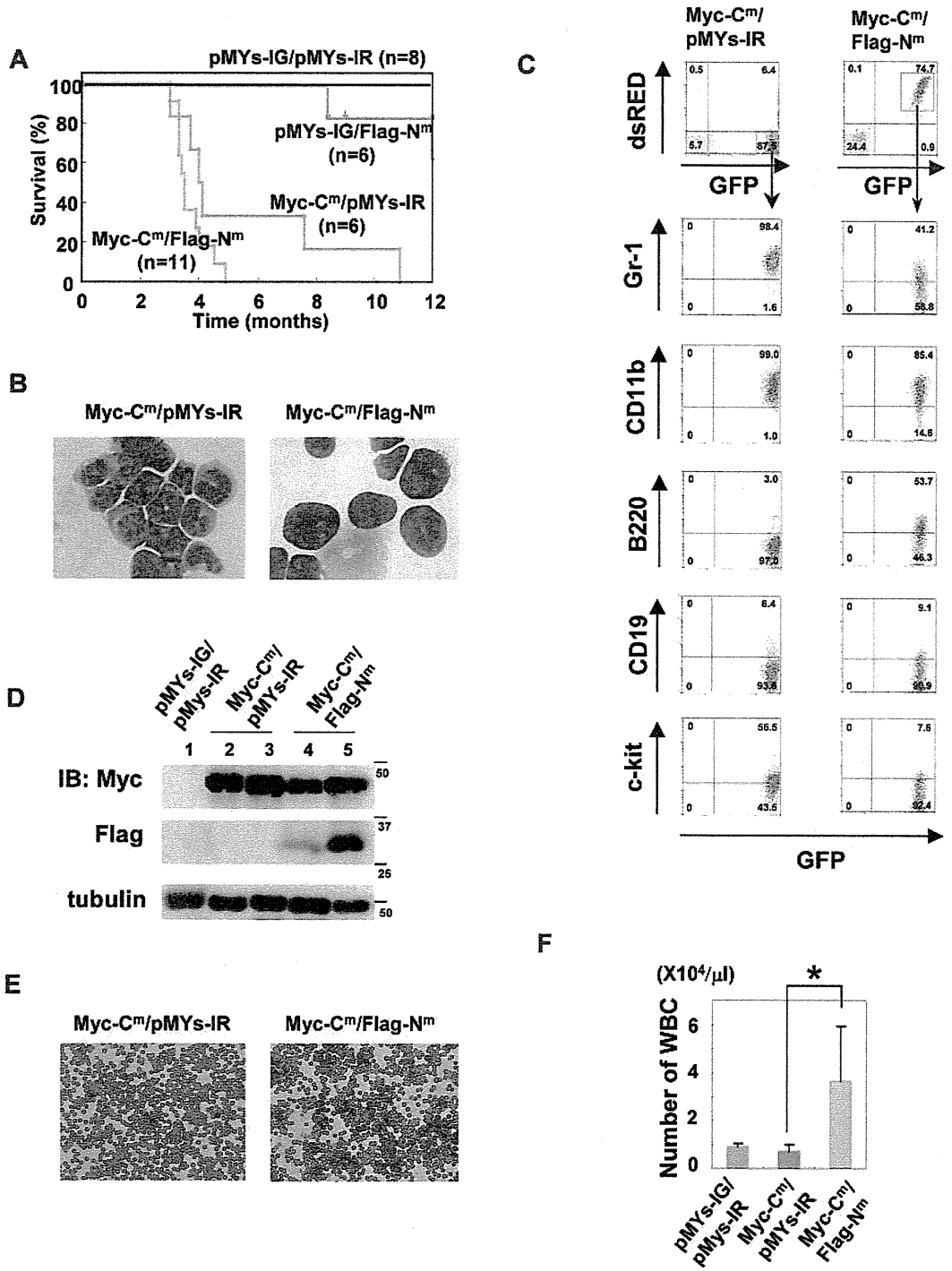

Figure 5. Coexpression of both C/EBPα-C^m and C/EBPα-N^m led to AML with leukocytosis with shorter latencies. (A) Kaplan-Meier analysis for the survival of mice that received transplants of BM cells transduced with both Myc-tagged C/EBPα-C^m-IG and pMYs-IR (Myc-C^m/pMYs-IR, n = 6), both pMYs-IG and Flag-tagged C/EBPα-N^m-IR (pMYs-IG/Flag-N^m, n = 6), both Myc-tagged C/EBPα-C^m-IG and Flag-tagged C/EBPα-N^m-IR (Myc-C^m/Flag-N^m, n = 11), or mock (pMYs-IG/pMYs-IR, n = 8). (B) Cytospin preparations of BM cells derived from mice/My-C^m/pMYs-IR or mice/Myc-C^m/Flag-N^m were stained with Giemsa. A representative photograph is shown. Images were obtained with a BX51 microscope and a DP12 camera (Olympus); objective lens, UplanFl (Olympus); original magnification ×100. (C) Flow cytometric analysis of BM cells derived from mice/Myc-C^m/pMYs-IR (left) or mice/Myc-C^m/Flag-N^m (right). The dot plots show expression of dsRED versus expression of GFP (1st panel). In the indicated gating, the dot plots show expression of Gr-1, CD11b, B220, CD19, or c-kit labeled with phycoerythrin-Cy5–conjugated streptavidin versus expression of GFP. (D) Expression of Myc-tagged C/EBPα-C^m protein and p30 protein generated by Flag-tagged C/EBPα-N^m in BM cells derived from mice/pMYs-IG/pMYs-IR (lane 1), mice/Myc-C^m/pMYs-IR (lanes 2-3), or mice/Myc-C^m/Flag-N^m (lanes 4-5) was detected by using anti-Myc monoclonal Ab (top) and ant-Flag mAb (middle), respectively, in Western blot analysis. Equal loading was evaluated by probing the immunoblots with anti-tubulin Ab (bottom). Data are representative of 3 independent experiments. (E) Peripheral blood smears obtained from mice/Myc-C^m/pMYs-IR (left) or mice/Myc-C^m/Flag-N^m (right) were stained with Giemsa. Images were obtained with a BX51 microscope and a DP12 camera (Olympus); objective lens, UplanFl (Olympus); original magnification ×20. (F) Counts of white blood cells (WBC) obtained from mice/Myc-C^m/pMYs-IR (n = 6), mice/Myc-C^m/Flag-N^m (n = 8), or mice/pMYs-IG/pMYs-IR (n = 8). All data points correspond to the mean and the standard deviation (SD). Statistically significant differences are shown. *$P < .05$.

reported that PU.1 plays important roles in macrophage differentiation, which is hampered by its interaction with C/EBPα through its C-terminal bZIP domain,[50] we investigated whether PU.1 plays some role in C/EBPα-C^m–mediated transcription. The present

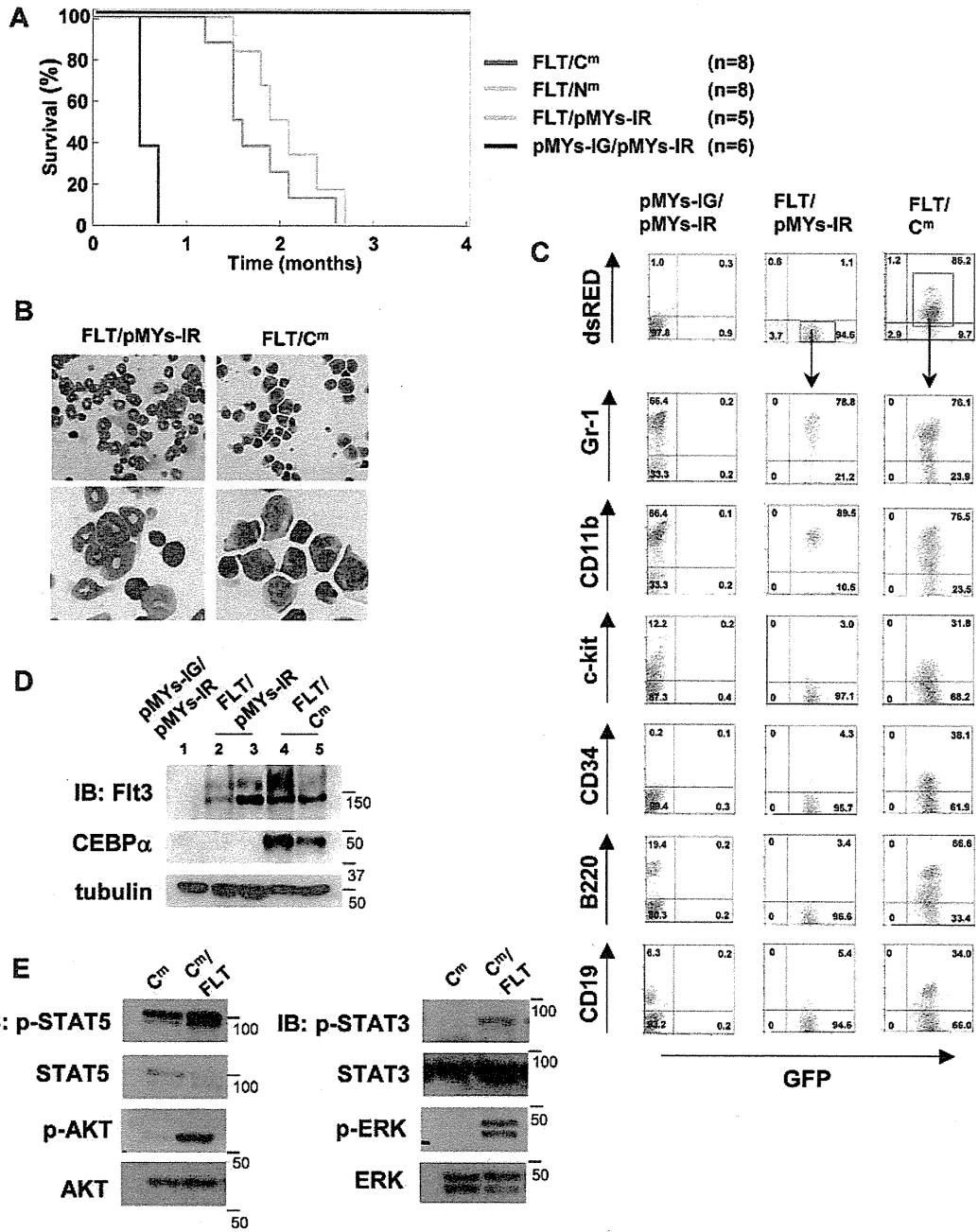

Figure 6. C/EBPα-C^m, but not C/EBPα-N^m, collaborated with Flt3-ITD in inducing aggressive AML. (A) Kaplan-Meier analysis for the survival of mice that received transplants of BM cells transduced with both Flt3-ITD-IG and pMYs-IR (FLT/pMYs-IR, n = 5), both Flt3-ITD-IG and C/EBPα-C^m-IR (FLT/C^m, n = 8), both Flt3-ITD-IG and C/EBPα-N^m-IR (FLT/N^m, n = 8), or mock (pMYs-IG/pMYs-IR, n = 8). (B) Cytospin preparations of BM cells derived from mice/FLT/pMYs-IR or mice/FLT/C^m were stained with Giemsa. Images were obtained with a BX51 microscope and a DP12 camera (Olympus); objective lens, UplanFl (Olympus); original magnification ×40 (top), ×100 (bottom). (C) Flow cytometric analysis of BM cells derived from mice/pMYs-IG/pMYs-IR, mice/FLT/pMYs-IR, or mice/FLT/C^m. The dot plots show expression of dsRED versus expression of GFP (first panel). In the indicated gating, the dot plots show expression of Gr-1, CD11b, c-kit, CD34, B220, or CD19 labeled with phycoerythrin-Cy5–conjugated streptavidin versus expression of GFP. (D) Expression of C/EBPα-C^m or Flt3-ITD in spleen cells of mice/pMYs-IG/pMYs-IR (lane 1), mice/FLT/pMYs-IG (lanes 2-3), or mice/FLT/C^m (lanes 4-5) was detected by using anti-C/EBPα (14AA) Ab (middle) or anti-Flt3 Ab (top), respectively, in Western blot analysis. Equal loading was evaluated by probing the immunoblots with anti-tubulin Ab. Data are representative of 3 independent experiments. (E) Immortalized leukemic cells derived from mice/FLT/C^m had increased phosphorylation of STAT5, AKT, STAT3, and ERK compared with those from mice/C^m. Whole-cell extracts of the former cells (immortalized in the absence of IL-3) or the latter (immortalized in the presence of IL-3) were immunoblotted with phospho-specific Abs as described in the Methods. Equal loading was evaluated by reprobing the immunoblots with anti-STAT5, anti-AKT, anti-STAT3, or anti-ERK Abs. Data are representative of 3 independent experiments.

result indicated that C/EBPα synergized with exogenously expressed PU.1 in stimulating transcription of the target genes in 293T cells, which was profoundly inhibited by C/EBPα-C^m but not by C/EBPα-N^m (Figure 2B), and suggested that C/EBPα-C^m hampers PU.1 from interacting with other molecules including C/EBPα in hemopoietic cells, leading to inhibition of granulocytic differentiation.

As for cooperation between C/EBPα-N^m and C/EBPα-C^m in leukemogenesis, we demonstrated using BMT models that C/EBPα-N^m and C/EBPα-C^m in combination induced AML with shorter latencies compared with transplantation of C/EBPα-C^m–transduced BM cells alone. In addition, combining both mutations resulted in increased number of leukemic cells, implicating C/EBPα-N^m in expansion of the cells whose differentiation was

blocked by C/EBPα-C^m. Thus, these results suggested that C/EBPα-C^m works as a class II mutation while C/EBPα-N^m works as a class I mutation in inducing leukemia.[31-36] To test this hypothesis, we built another BMT model where BM cells transduced with Flt3-ITD and either C/EBPα-C^m or C/EBPα-N^m were transplanted to lethally irradiated mice. Flt3-ITD dramatically shortened the latency of leukemia induced by C/EBPα-C^m but not by C/EBPα-N^m, indicating that C/EBPα-C^m worked as a class II mutation in inducing leukemia. Transplantation of BM cells transduced with both C/EBPα-C^m and Flt3-ITD quickly induced leukemia in just 2 weeks after transplantation. Most of the transplanted mice seemed to develop biphenotypic leukemia as assessed on the morphology and surface marker expressions (Figure 6B-C). In our hands, BM cells transduced with Flt3-ITD sometimes induce lymphoid malignancies in addition to myeloproliferative disease,[49] bringing some complexity to the experiment. Nonetheless, dramatically shortened latencies with the combination of C/EBPα-C^m and Flt3-ITD strongly indicated that C/EBPα-C^m works as a class II mutation in inducing leukemia. On the other hand, because the expression levels of C/EBPα-N^m was low in our experiments, further experiments will be required to firmly demonstrate that C/EBPα-N^m plays a class I-like role. One possible experiment is to test a combination between C/EBPα-N^m and a known class II mutation. Nonetheless, a class I-like role of C/EBPα-N^m was suggested by the marked increase in the number of leukemic cells in mice/Myc-C^m/Flag-N^m compared with mice/Myc-C^m/pMYs-IR. In relation to this, although the "2-hit theory" well explain many clinical observations, additional classes of mutations may be required for the comprehensive understanding of leukemogenesis as proposed by Renneville et al[32] In fact, we detected more than 3 mutations including mutations, chromosomal translocations, or deletions in 5 of 20 patients with leukemia and MDS (Table 1).

Concerning the in vivo effects of *CEBPA* mutations, several different results were reported.[29,30,51-54] Bereshchenko et al[30] have recently published a report using knock-in mice that C/EBPα-p30 and a C-terminal mutation collaborated in inducing leukemia. Our results basically agreed with those by Bereshchenko et al. However, while our results implicated C-terminal mutations of C/EBPα in differentiation, leading to leukemia with relatively long latencies, Bereshchenko et al[30] suggested premalignant HSC expansion by C-terminal mutations. The reason for the disparity is not clear, but was partly caused by the difference in the strength or functions of different C-terminal mutants or in the expression levels of mutants in knock-in mice and BMT models. Concerning the experimental systems, knock-in mice are superior to mouse BMT models in several aspects as indicated previously.[29,30] Most importantly, expression of the mutant C/EBPα is driven by the authentic promoter in knock-in mice while it is over-driven by an external promoter in BMT models. Moreover, replacement of both alleles with different C/EBPα mutations closely mimics human leukemia, as it lacks the WT C/EBPα unlike the BMT model. In addition, in BMT models, retrovirus integration sites sometimes modify the phenotype of the disease. However, BMT models do have some advantages. First, in contrast to knock-in mice where all hemopoietic cells express the mutant allele, only some cells can be of a leukemia origin, which would more faithfully mimic human pathologic situations. In addition, various mutants can be readily tested in vivo. Bereshchenko et al[30] used K313dup as a C-terminal *CEBPA* mutation, demonstrating that mice$^{K313dup/+}$ did not develop leukemia. K313dup was a weak inducer of leukemia in our BMT model, where only 1 of the 4 transplanted mice developed myeloid leukemia in 10 months (data not shown). On the other hand, C/EBPα-C^m, a C-terminal mutation with 304-323dup that we used in the present study, induced leukemia in most transplanted mice (Figure 4A). Thus, knock-in mice models and BMT models can complement with each other in investigating in vivo leukemogenesis.

To summarize, we have presented a series of evidence, including clinical data, in vitro experiments, and mouse BMT models, showing that 2 different mutations of *CEBPA*, C/EBPα-N^m and C/EBPα-C^m, play distinct roles in leukemogenesis. Moreover, our results strongly indicated that C/EBPα-C^m is able to play as a class II mutation in concert with Flt3-ITD in inducing leukemia. Further elucidation of the molecular mechanism of *CEBPA* mutations–induced leukemia may pave a novel way to treating patients with leukemia.

Acknowledgments

We thank Dr Atsushi Iwama, Dr Claus Nerlov, and Dr Shigekazu Nagata for kindly providing plasmids. We are grateful to Dr Dovie Wylie for her excellent editing of the English.

This work was supported by the Ministry of Education, Science, Technology, Sports and Culture, Japan and in part supported by Global COE Program "Center of Education and Research for the Advanced Genome-Based Medicine, for personalized medicine and the control of worldwide infectious diseases," MEXT, Japan.

Authorship

Contribution: N.K. did all the experiments and participated in writing the manuscript; J.K. oversaw all the experiments and actively participated in manuscript writing; N.D., Y.K., N.W.O., K.T., F.N., T.O., and Y.E. technically supported BMT; Y.F. and H.N. provided plasmids and reagents; Y.H. and H.H. provided and analyzed human samples; and T.K. conceived the project, secured funding, and actively participated in manuscript writing.

Conflict-of-interest disclosure: T.K. serves as a consultant for R&D Systems. The remaining authors declare no competing financial interests.

Correspondence: Toshio Kitamura, Division of Cellular Therapy and Division of Stem Cell Signaling, The Institute of Medical Science, The University of Tokyo, 4-6-1 Shirokanedai, Minato-ku, Tokyo 108-8639, Japan; e-mail: kitamura@ims.u-tokyo.ac.jp.

References

1. Zhang P, Iwasaki-Arai J, Iwasaki H, et al. Enhancement of hematopoietic stem cell repopulating capacity and self-renewal in the absence of the transcription factor C/EBP alpha. *Immunity.* 2004;21(6):853-863.
2. Tenen DG, Hromas R, Licht JD, Zhang D-E. Transcription factors, normal myeloid development, and leukemia. *Blood.* 1997;90(2):489-519.
3. Friedman AD, McKnight SL. Identification of two polypeptide segments of CCAAT/enhancer-binding protein required for transcriptional activation of the serum albumin gene. *Genes Dev.* 1990;4(8):1416-1426.
4. Landschulz WH, Johnson PF, McKnight SL. The DNA binding domain of the rat liver nuclear protein C/EBP is bipartite. *Science.* 1989;243(4899):1681-1688.
5. Nerlov C, Ziff EB. CCAAT/enhancer binding protein-alpha amino acid motifs with dual TBP and TFIIB binding ability co-operate to activate transcription in both yeast and mammalian cells. *Embo J.* 1995;14(17):4318-4328.
6. Lin FT, MacDougald OA, Diehl AM, Lane MD. A 30-kDa alternative translation product of the CCAAT/enhancer binding protein alpha message:

Napsin A, a New Marker for Lung Adenocarcinoma, Is Complementary and More Sensitive and Specific Than Thyroid Transcription Factor 1 in the Differential Diagnosis of Primary Pulmonary Carcinoma

Evaluation of 1674 Cases by Tissue Microarray

Bradley M. Turner, MD, MPH, MHA; Philip T. Cagle, MD; Irma M. Sainz, MD; Junya Fukuoka, MD, PhD; Steven S. Shen, MD, PhD; Jaishree Jagirdar, MD

• ***Context.***—**Differentiation of non–small cell carcinoma into histologic types is important because of new, successful therapies that target lung adenocarcinoma (ACA). TTF-1 is a favored marker for lung ACA but has limited sensitivity and specificity. Napsin A (Nap-A) is a functional aspartic proteinase that may be an alternative marker for primary lung ACA.**

Objectives.—**To compare Nap-A versus TTF-1 in the typing of primary lung carcinoma and the differentiation of primary lung ACA from carcinomas of other sites.**

Design.—**Immunohistochemistry for Nap-A and TTF-1 was performed on tissue microarrays of 1674 cases of carcinoma: 303 primary lung ACAs (18.1%), 200 primary squamous cell lung carcinomas (11.9%), 52 primary small cell carcinomas of the lung (3.1%), and carcinomas of the kidney (n = 320; 19.1%), thyroid (n = 96; 5.7%), biliary (n = 89; 5.3%), bladder (n = 47; 2.8%), breast (n = 93; 5.6%), colon (n = 95; 5.7%), liver (n = 96; 5.7%), ovaries (n = 45; 2.7%), pancreas (n = 48; 2.9%), prostate (n = 49; 2.9%), stomach (n = 93; 5.6%), and uterus (n = 48; 2.9%). Cases were evaluated against a negative control as negative, weak positive, and strong positive.**

Results.—**Nap-A was more sensitive than TTF-1 for primary lung ACA (87% versus 64%; $P < .001$). Nap-A was more specific than TTF-1 for primary lung ACA versus all tumors, excluding kidney, independent of tumor type ($P < .001$).**

Conclusions.—**Nap-A is superior to TTF-1 in distinguishing primary lung ACA from other carcinomas (except kidney), particularly primary lung small cell carcinoma, and primary thyroid carcinoma. A combination of Nap-A and TTF-1 is useful in the distinction of primary lung ACA (Nap-A$^+$, TTF-1$^+$) from primary lung squamous cell carcinoma (Nap-A$^-$, TTF-1$^-$) and primary lung small cell carcinoma (Nap-A$^-$, TTF-1$^+$).**

(*Arch Pathol Lab Med.* 2012;136:163–171; doi: 10.5858/arpa.2011-0320-OA)

Lung cancer is the most frequently diagnosed cancer and the leading cause of cancer mortality in the world.[1,2] Most lung cancers are in advanced stages when first detected, with a 5-year survival rate of 14%.[2,3] Primary pulmonary tumors consist of several histologic types, most of which can be classified as malignant epithelial tumors. Of these malignant epithelial tumors, most are commonly classified as non–small cell lung carcinomas (NSCLCs) and as small cell carcinomas (SCCs). Non–small cell lung carcinoma accounts for approximately 80% of all lung cancers, with SCC accounting for most of the rest.[2,4] Traditionally, the most common NSCLC consists of adenocarcinoma (≥40%) and squamous cell carcinoma (30%).[1,2,4] Previously, it was sufficient to diagnosis primary lung carcinoma as either NSCLC or SCC for treatment purposes. With the development of new, successful treatments for adenocarcinoma, it is essential to diagnose the type of NSCLC whenever possible. These new treatments include (1) therapies that target *EGFR* mutations and *ALK* fusion genes that are found almost exclusively in adenocarcinomas; (2) bevacizumab (monoclonal antibody to *VEGF*), which is effective as a first-line agent in many adenocarcinomas but may cause severe, even life-threatening, hemorrhage in patients with squamous cell carcinoma; and (3) pemetrexed (new antifolate agent) may be effective in adenocarcinomas but is not effective in squamous cell carcinomas.[5–9] The lung is also a common site of metastases from other sites, including breast, gastrointestinal tract, and genitourinary tract. Metastatic adenocarcinoma of an unknown primary

Accepted for publication June 28, 2011.

From the Department of Pathology, University of Texas Health Science Center, San Antonio, Texas (Drs Turner and Jagirdar); the Department of Pathology, Weill College of Medicine Cornell University, The Methodist Hospital, Houston, Texas (Drs Cagle and Shen); the Department of Pathology, Nacogdoches Memorial Hospital, Nacogdoches, Texas (Dr Sainz); and the Laboratory of Pathology, Toyama University Hospital, Toyama, Japan (Dr Fukuoka).

The authors have no relevant financial interest in the products or companies described in this article.

Reprints: Jaishree Jagirdar, MD, Department of Pathology, University of Texas Health Science Center, 7703 Floyd Curl Drive, San Antonio, TX 78230 (e-mail: Jagirdar@uthscsa.edu).

accounts for approximately 3% to 5% of all malignant neoplasms and, as such, is one of the 10 most-frequently diagnosed cancers in humans.[10,11]

Routine sections stained with hematoxylin-eosin remain the most-common method by which lung cancers are classified; however, typing of NSCLC and the more poorly differentiated tumors is often hard to achieve by hematoxylin-eosin alone.[1,12,13] Immunohistochemistry has emerged as a powerful, adjunctive tool for the differential diagnosis of lung carcinomas, whether primary or secondary to the lung. The most-useful application is in distinguishing primary lung tumors from metastatic tumors to the lung from common sites (colon, breast, prostate, pancreas, stomach, kidney, bladder, ovaries, and uterus). Although there is currently no "lung-specific tumor marker," continued efforts to identify such a marker are scattered throughout the literature. Although progenitor stem-cell markers are being hypothesized as an immunohistochemical method to differentiate pulmonary carcinomas, that has not been well established.[14] With the help of a relatively restricted marker, thyroid transcription factor 1 (TTF-1), it is possible to separate a lung primary from a metastasis with a reasonable degree of certainty. Another lung-specific marker on the horizon is napsin A (Nap-A), which appears to complement TTF-1 in defining a primary lung carcinoma,[15] also appears to be helpful in subtyping NSCLC, and may be helpful in distinguishing NSCLC, particularly poorly differentiated adenocarcinoma, from SCC.[1]

TTF-1 is identified as a *nuclear* tissue-specific, 38-kDa, homeodomain protein containing DNA-binding activity. TTF-1 regulates gene expression in the thyroid, lungs, and diencephalon during embryogenesis. It is expressed in follicular cells of the thyroid, in areas of the developing brain, in type II pneumocytes, and in nonciliated bronchiolar epithelial cells.[16] In the lung, TTF-1 is responsible for transcriptional activation of surfactant proteins A, B, and C and Clara cell secretory proteins. Neoplasms of pulmonary origin have been found to retain variable TTF-1 expression according to histologic type.[1,15,17] Antibodies against TTF-1 antigen are well established for the differentiation between primary lung adenocarcinomas and adenocarcinomas from other sites; however, sensitivities as low as 54% in primary lung adenocarcinoma have been reported.[18] TTF-1 results are also positive in 7% to 10% of primary squamous cell carcinomas of the lung.[19–25] In addition, TTF-1 positivity is not universally specific to the lung. TTF-1 positivity is seen in up to 100% of primary thyroid carcinomas and in up to 90% of small cell carcinomas of any origin.[19–27]

Napsin A is a functional aspartic proteinase, expressed in the *cytoplasm* of healthy lung parenchyma. It is homologous with the polypeptide TAO2 and involved in maturation of the biologically active surfactant protein B. It also consists of a 38-kDa protein, a single-chain protein expressed in type II pneumocytes, alveolar macrophages, renal tubules, and exocrine glands and ducts in the pancreas.[18,28,29] It is involved in the N-terminal and C-terminal maturation of prosurfactant protein B in type II pneumocytes.[30] Earlier, we demonstrated that Nap-A is expressed in primary lung carcinomas and facilitates the differentiation between primary lung carcinomas and metastatic lesions.[15] Positive immunoreactivity is seen as usually intense, granular cytoplasmic staining.[1,31] Other studies have shown that Nap-A is more sensitive than TTF-1 in distinguishing lung primary from other adenocarcinomas.[18,31,32]

In this study, we compared Nap-A with TTF-1 in an effort to distinguish primary lung carcinoma from tumors of other organ sites, to better subtype NSCLC, and to help distinguish primary NSCLC from primary lung SCC. We used tissue microarrays to examine the staining patterns of 1674 primary carcinomas with Nap-A and TTF-1. The carcinoma types included bile duct, bladder, breast, colon, kidney, liver, lung (adenocarcinoma, squamous cell carcinoma, and small cell carcinoma), ovaries, pancreas, prostate, stomach, thyroid, and uterus. To our knowledge, our study is the largest study to date examining the sensitivity of Nap-A, compared with TTF-1, in primary lung adenocarcinoma and the largest study to date examining the expression of Nap-A in primary lung SCC.

MATERIALS AND METHODS

Histology

A total of 1674 tumor sections were processed in triplicate. Tissues studied were obtained from 2 sources. The first group of tissues studied was made available by the Laboratory of Pathology at Toyama University Hospital (Toyama, Japan). Paraffin sections (6 μm) from primary carcinomas of the bile ducts (n = 89; 5.3%), bladder (n = 47; 2.8%), breast (n = 93; 5.6%), colon (n = 95; 5.7%), kidney (n = 93; 5.6%), liver (n = 96; 5.7%), lung (n = 188; 11.2%; squamous cell [n = 94; 5.6%] and adenocarcinoma [n = 94; 5.6%]), ovaries (n = 45; 2.7%), pancreas (n = 48; 2.9%), prostate (n = 49; 2.9%), stomach (n = 93; 5.6%), thyroid (n = 96; 5.7%), and uterus (n = 48; 2.9%) were selected. A second group of tissues to be studied were made available from Weill College of Medicine Cornell University, The Methodist Hospital (Houston, Texas). These included primary lung tumors (n = 338; 20.2%; adenocarcinoma [n = 209; 12.5%], squamous cell carcinoma [n = 106; 6.3%], and small cell carcinoma [n = 23; 1.4%]), a separate set of small cell carcinomas of the lung (n = 29; 1.7%), and renal tumors (n = 227; 13.6%). The samples studied were originally fixed in 10% formalin for periods ranging from 1 to 7 days. Tissue microarrays in triplicate were constructed according to standard protocols[33] using a dedicated tissue microarray instrument (Beecher TMA, Beecher instruments, Sun Prairie, Wisconsin).

Immunohistochemistry

Immunohistochemistry was performed at the immunohistochemistry laboratory at the University of Texas Health Science Center (San Antonio, Texas). Antibodies used included anti-human Nap-A mouse immunoglobulin G (IgG) monoclonal antibody (TMU-Ad02, 1:100; Immuno-Biological Laboratories Co, Ltd, Takasaki, Japan) and anti-rat TTF-1 mouse IgG monoclonal antibody, known to react with human TTF-1 (8G7G3/1,[1] 1:80; DakoCytomation Inc, Carpinteria, California). Protocols, reagents for antigen retrieval (Reveal Decloaker 10×), and the detection system were from Biocare Medical (Concord, California). Slides were stained with a Ventana Immunostainer (Ventana Medical Systems, Tucson, Arizona). Both Nap-A and TTF-1 immunostaining were performed on the first group of tissue specimens (from Toyama University Hospital). Only Nap-A immunostaining was performed on the second group of tissue specimens (from Weill College of Medicine). After staining, the tissue microarrays were scanned with a Spectrum/Spectrum Plus (Aperio Technologies, Inc; Bristol, United Kingdom) to a dedicated server and were analyzed by 3 pathologists independently. Staining intensity was evaluated as follows: negative, no staining to minimal light-brown to dust; weak positive, minimal, patchy, or diffuse cytoplasmic staining for Nap-A or nuclear staining for TTF-1; and strong positive, moderate to intense-brown, granular, cytoplasmic staining for Nap-A or nuclear staining for TTF-1. All results were evaluated relative to a negative control of the same tumor.

Table 1. Number and Percentage of Positive-Staining Tumors for Napsin A (Nap-A)[a] and Thyroid Transcription Factor 1 (TTF-1)[b] Categorized by Tumor Type

Tumor	Total Tested With Nap-A, No.	Nap-A, No. (% Positive)	Total Tested With TTF-1, No.	TTF-1, No. (% Positive)
Lung	555			
Adenocarcinoma	303	264 (87)	94	60 (64)
Squamous cell carcinoma	200	5 (3)	94	2 (2)
Small cell carcinoma	52	0 (0)		(90)[b]
Renal	320	181 (57)	93	2 (2)
Papillary	108	78 (72)		N/A
Conventional[c]	196	101 (52)		N/A
Other[d]	16	2 (13)		N/A
Thyroid	96	7 (7)	96	77 (80)
Other	703	21 (3)	703	6 (1)
Bile duct	89	2 (2)	89	1 (1)
Bladder	47	0 (0)	47	0 (0)
Breast	93	3 (3)	93	1 (1)
Colon	95	2 (2)	95	0 (0)
Liver	96	5 (5)	96	2 (2)
Ovaries	45	3 (6)	45	1 (1)
Pancreas	48	2 (4)	48	0 (0)
Prostate	49	0 (0)	49	0 (0)
Stomach	93	0 (0)	93	0 (0)
Uterus	48	4 (8)	48	1 (2)
Total	**1674**		**1080**	

[a] All 52 primary lung small cell carcinomas were negative for Nap-A in our study group.
[b] Primary lung small cell carcinoma tissues were not tested with TTF-1. The TTF-1 profile of primary lung small cell carcinoma was gleaned from the literature (90% of primary lung small cell carcinomas are positive for TTF-1).[19-27]
[c] Defined as composed of either clear cells or granular cells or both.
[d] Includes 13 urothelial type and 3 chromophobe type. The 2 positive staining tumors were both chromophobe types.

Statistical Methods

The χ^2 statistic and the Fisher exact (FE) test were used to investigate whether distributions of categoric variables differ from one another. Sensitivity, specificity, positive predictive value (PPV), negative predictive value (NPV), positive likelihood ratio (PLR), and negative likelihood ratio (NLR) were calculated in the usual format. If the ratio of the number of patients in disease group 1 and the number of patients in disease group 2 were not equivalent, PLR [$PLR = sensitivity/(1 - specificity)$] and NLR [$NLR = (1 - sensitivity)/specificity$] may be a better indicator of the proportion of patients with positive or negative test results who are correctly diagnosed because likelihood ratios do not depend on prevalence. Likelihood ratios predict the probability of disease, given a positive (PLR) or negative (NLR) test result.[34] Data in the Tables are presented as the number of positive staining tumors versus the number of negative staining tumors in the same tumor type for Nap-A versus TTF-1 or as the number of positive staining tumors versus the number of negative staining tumors in different tumor types for Nap-A or TTF-1 alone.

RESULTS

The results of immunohistochemistry for Nap-A and TTF-1 are summarized in Table 1. Tables 2 through 6 show the sensitivity, specificity, PPV, NPV, PLR, and NLR of Nap-A and TTF-1 in primary lung adenocarcinoma relative to various tumor types. Positive immunoreactivity (sensitivity) was seen in 264 of 303 pulmonary adenocarcinomas (87.1%) for Nap-A, compared with 60 of 94 pulmonary adenocarcinomas (64%) for TTF-1 ($P < .001$ χ^2 test; Tables 1 and 3); 24 of 84 primary pulmonary adenocarcinomas (28.6%) detected by Nap-A were missed on TTF-1 staining (Table 2). Excluding renal carcinomas, comparison of the number of cases staining positive with Nap-A in pulmonary adenocarcinoma versus all other tumors shows a significant difference ($P < .001$ χ^2 and FE tests), independent of tumor type (Tables 1 and 3). All of the nonpulmonary adenocarcinomas displayed a weak-positive staining pattern (relative to the negative control), compared with a strong-positive staining in the pulmonary adenocarcinomas (Figure 1, A through D). Table 3 also shows that the specificity of Nap-A for primary lung carcinoma was 97% (compared with 90% for TTF-1), NPV was 96% (equal to TTF-1, although with a lower NLR), and PPV (PLR) was 89% (27.75), compared with 41% (6.71) for TTF-1. The likelihood ratios may be better comparative indicators in these results than are the predictive values (see "Statistical Methods"). Both markers showed decreased positive immunostaining with more poorly differentiated adenocarcinomas, consistent with previous studies.[1] Positive immunoreactivity for Nap-A was only seen in 7 of 96 thyroid carcinomas (7%) for Nap-A, compared with 77 of 96 thyroid carcinomas (80%) for TTF-1 ($P < .001$ χ^2 test; Tables 1 and 4). All the positive thyroid tumors were of the papillary type, and all displayed a weak-positive staining pattern (Figure 2, A) relative to the negative control (Figure 2, B). Comparison of the number of cases staining with Nap-A in pulmonary adenocarcinoma versus thyroid carcinoma shows a significant difference ($P < .001$ χ^2 test). When comparing only primary lung adenocarcinoma

Table 2. Napsin A (Nap-A) and Thyroid Transcription Factor 1 (TTF-1) Staining in Primary Lung Adenocarcinoma

Test Result	Nap-A Positive, No.	Nap-A Negative, No.
TTF-1 positive	60	0
TTF-1 negative	24	10
Total	**84**	**10**

Table 3. Napsin A (Nap-A) and Thyroid Transcription Factor 1 (TTF-1) Sensitivity, Specificity, Predictive Value (PV), and Likelihood Ratio (LR) for Primary Lung Adenocarcinoma Versus Other Tumors					
Stain Results	**Lung Adenocarcinoma, No.**	**Other,[a] No.**	**Total**	**PV, % (PPV or NPV)**	**LR,[b] Result (PLR or NLR)**
Nap-A$^+$	264	33	**297**	89 (PPV)	27.75 (PLR)
Nap-A$^-$	39	1018	**1057**	96 (NPV)	0.13 (NLR)
Total	**303**	**1051**	**1354**		
	Sensitivity, 87%	Specificity, 97%			
TTF-1$^+$	60	85	**145**	41 (PPV)	6.71 (PLR)
TTF-1$^-$	34	808	**842**	96 (NPV)	0.40 (NLR)
Total	**94**	**893**	**987**		
	Sensitivity, 64%	Specificity, 90%			

Abbreviations: NLR, negative likelihood ratio; NPV, negative predictive value; PLR, positive likelihood ratio; PPV, positive predictive value.

[a] The "Other" group includes all remaining tumors tested, except renal cell carcinoma (squamous cell carcinoma, small cell carcinoma, thyroid, bile duct, bladder, breast, colon, liver, ovaries, pancreas, prostate, stomach, uterus).

[b] Likelihood ratios may be better comparative indicators here than are predictive values (see "Statistical Methods" in text).

versus thyroid carcinoma (Table 4), the specificity for lung carcinoma was 93%, compared with 20% for TTF-1; NPV (NLR) was 70% (0.14), compared with 36% (1.83) for TTF-1; and PPV (PLR) was 97% (11.95), compared with 44% (0.80) for TTF-1. Again, the likelihood ratios may be better comparative indicators here than are the predictive values (see "Statistical Methods"). No immunoreactivity was seen for Nap-A in our sample of small cell carcinomas ($P < .001$

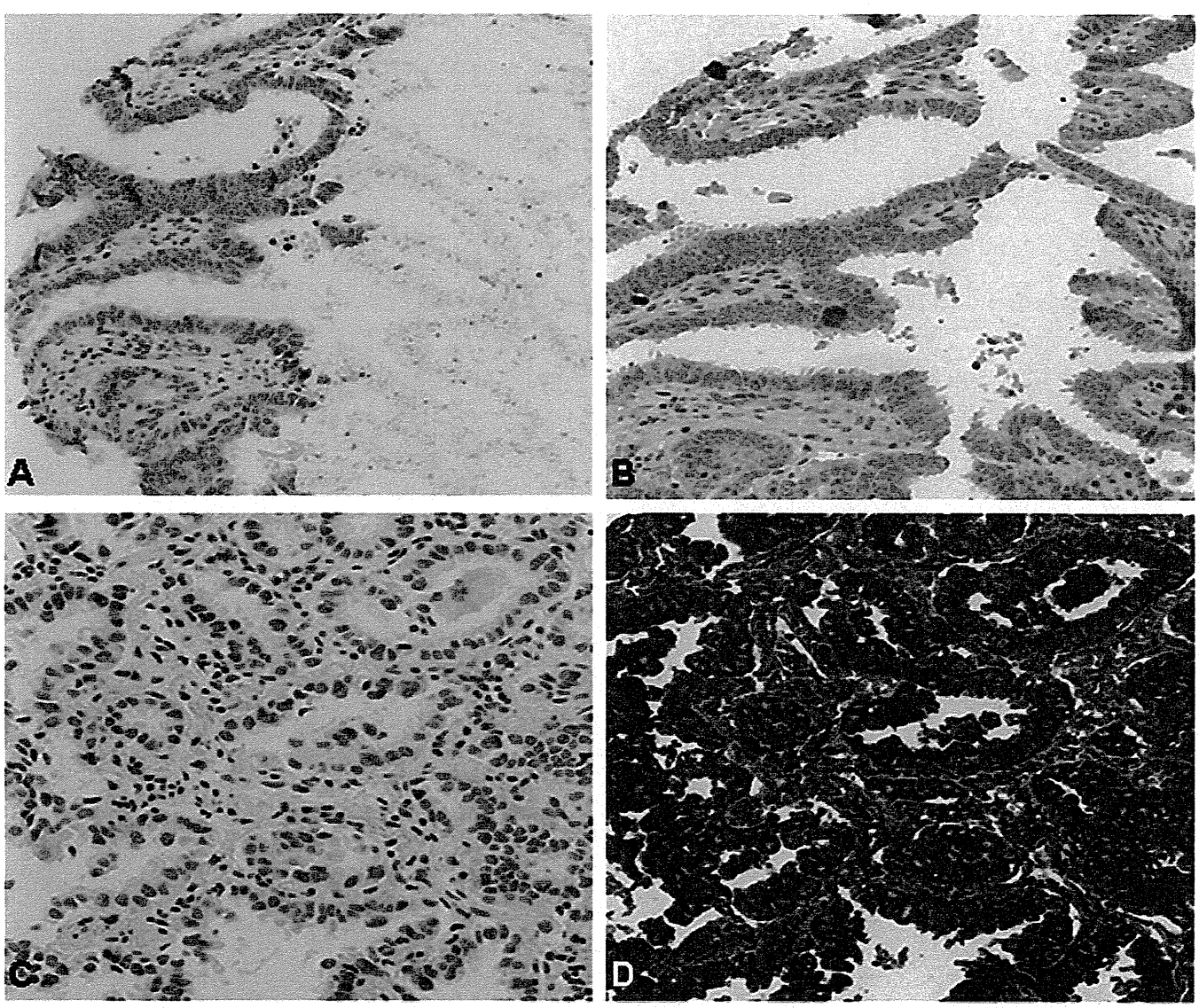

Figure 1. *Napsin A. A, Negative control, uterine adenocarcinoma. B, Positive staining in uterine adenocarcinoma. C, Negative control, pulmonary adenocarcinoma. D, Positive staining in pulmonary adenocarcinoma. Note the background staining in the negative uterine adenocarcinoma control and the weak-positive staining in the tumor. Compare those results to the strong-positive staining in the pulmonary adenocarcinoma against a "cleaner" negative control (original magnifications ×20 [A through D]).*

Table 4. Napsin A (Nap-A) and Thyroid Transcription Factor 1 (TTF-1) Sensitivity, Specificity, Predictive Value (PV), and Likelihood Ratio (LR) for Primary Lung Adenocarcinoma Versus Primary Thyroid Carcinoma

Stain Result	Lung Adenocarcinoma, No.	Thyroid Carcinoma, No.	Total, No.	PV, % (PPV or NPV)	LR,[a] Result (PLR or NLR)
Nap-A$^+$	264	7	**271**	97 (PPV)	11.95 (PLR)
Nap-A$^-$	39	89	**128**	70 (NPV)	0.14 (NLR)
Total	**303**	**96**	**399**		
	Sensitivity, 87%	Specificity, 93%			
TTF-1$^+$	60	77	**137**	44 (PPV)	0.80 (PLR)
TTF-1$^-$	34	19	**53**	36 (NPV)	1.83 (NLR)
Total	**94**	**96**	**190**		
	Sensitivity, 64%	Specificity, 20%			

Abbreviations: NLR, negative likelihood ratio; NPV, negative predictive value; PLR, positive likelihood ratio; PPV, positive predictive value.

[a] Likelihood ratios may be better comparative indicators here than are predictive values (see "Statistical Methods" in text).

FE test; Table 5). Positive immunoreactivity was seen in only 5 of 200 primary pulmonary squamous cell carcinomas (2.5%) for Nap-A and in only 2 of 94 primary pulmonary squamous cell carcinomas (2%) for TTF-1 ($P > .99$ FE test; Table 6). All positive pulmonary squamous cell carcinomas showed weaker staining than the positive staining of pulmonary adenocarcinomas (Figure 3, A and B). Comparison of the number of cases (Table 1) staining positive with Nap-A in pulmonary adenocarcinoma versus renal carcinoma (57%) shows significant differences in papillary, conventional, and urothelial types ($P < .001$ χ^2 test) but not in the chromophobe type ($P = .34$ FE test) renal cell carcinomas. Again, all of the positive renal tumors displayed a weak-positive staining pattern (Figure 4, A) relative to the negative control (Figure 4, B). When comparing only primary lung adenocarcinoma versus renal cell carcinoma, specificity for lung carcinoma was 43%, NPV (NLR) was 78% (0.30), and PPV (PLR) was 59% (1.54). Inclusion of the renal carcinomas when comparing the number of cases staining positive with Nap-A in pulmonary adenocarcinoma versus all other tumors decreases the specificity and PPV (PLR) of primary lung adenocarcinoma to 84% and 55% (5.58), respectively, with the NPV (NLR) essentially unchanged (specificity, PPV [PLR], and NPV [NLR] of TTF-1 are also essentially unchanged).

COMMENT

Previous investigations of Nap-A have found that the sensitivity and specificity is at least equal to, and often greater than, that of TTF-1 in the identification of lung adenocarcinoma.[1,2,15,18,32] Most of these studies have had a relatively small number of cases (n = <100) and did not address the specificity, NPV, NLR, PPV, or PLR of Nap-A relative to other tumor types. None of the previous studies adequately addressed the issue of sensitivity, specificity, predictive values, or likelihood ratios when considering the subtyping of primary lung adenocarcinoma, particularly primary lung small cell carcinoma.

To our knowledge, we have the largest study to date demonstrating that Nap-A has a higher sensitivity, specificity, NPV, NLR, PPV, and PLR for primary pulmonary adenocarcinoma than TTF-1 has (Table 3); 24 of 84 primary pulmonary adenocarcinomas (28.6%) detected by Nap-A were missed with TTF-1 staining (Table 2). Furthermore, Nap-A is useful in distinguishing primary lung carcinoma from thyroid carcinoma, unlike TTF-1 (Table 4). In addition, Nap-A distinguished primary lung adenocarcinoma from primary small cell carcinoma with 100% specificity in our study (Table 5). The lack of Nap-A in pulmonary neuroendocrine tumors has been previously noted by Bishop et al,[1] but the number of cases in that work was too small to reach meaningful conclusions about its significance.[1] Our study confirms that Nap-A is a specific marker when considering a differential diagnosis between primary lung adenocarcinoma and small cell carcinoma. Although Nap-A and TTF-1 show similar specificity for primary lung adenocarcinoma when compared with primary lung squamous cell carcinoma, Nap-A may be better at predicting the presence or absence of disease with a positive or negative test, respectively (Table 6). Table 7 details the immunohistochemical profiles in our study of primary lung adenocarcinoma, primary lung squamous cell carcinoma, and primary lung small cell carcinoma. A combination of Nap-A and TTF-1 would be expected to be useful in the distinction of these 3 tumors (Table 8). Primary lung adenocarcinoma will likely exhibit Nap-A positivity (Nap-A$^+$) and will generally be TTF-1 positive (TTF-1$^+$), but may be TTF-1 negative (TTF-1$^-$). Primary lung squamous cell carcinoma will likely be negative for Nap-A (Nap-A$^-$) and TTF-1$^-$. Primary lung small cell carcinoma will likely be Nap-A$^-$ and TTF-1$^+$. Similar to Bishop et al,[1] we found that the Nap-A positivity decreased with more poorly differentiated lung tumors.

Two caveats deserve mention here, with an additional "caveat on the caveat." First, the specificity of Nap-A for primary lung carcinoma appears to be substantially challenged only when the differential diagnosis involves renal cell carcinoma, which is a relevant concern, given that a primary metastatic site for renal cell carcinoma is the lung.[35] Although there is a significant difference between the number of lung and renal tumors staining positive for Nap-A, the specificity, PPV, and PLR of Nap-A for primary lung adenocarcinoma, when examined against renal tumors only, is lower than it is when examined against other tumors. Although the clinical and radiographic history and the morphology should be adequate to distinguish the two, often the pathologist does not have that information. We agree with Bishop et al[1] that, when considering renal cell carcinoma in the differential diagnosis, a panel of additional immunohistochemical markers should be used. Initially, TTF-1 would be helpful to better distinguish primary lung from primary renal, and then, a subset of additional markers may be helpful in further subclassifying the renal tumor type. Secondly, although Nap-A is clearly more sensitive and specific than is TTF-1, when examined against thyroid carcinoma, the rare thyroid carcinoma that does stain

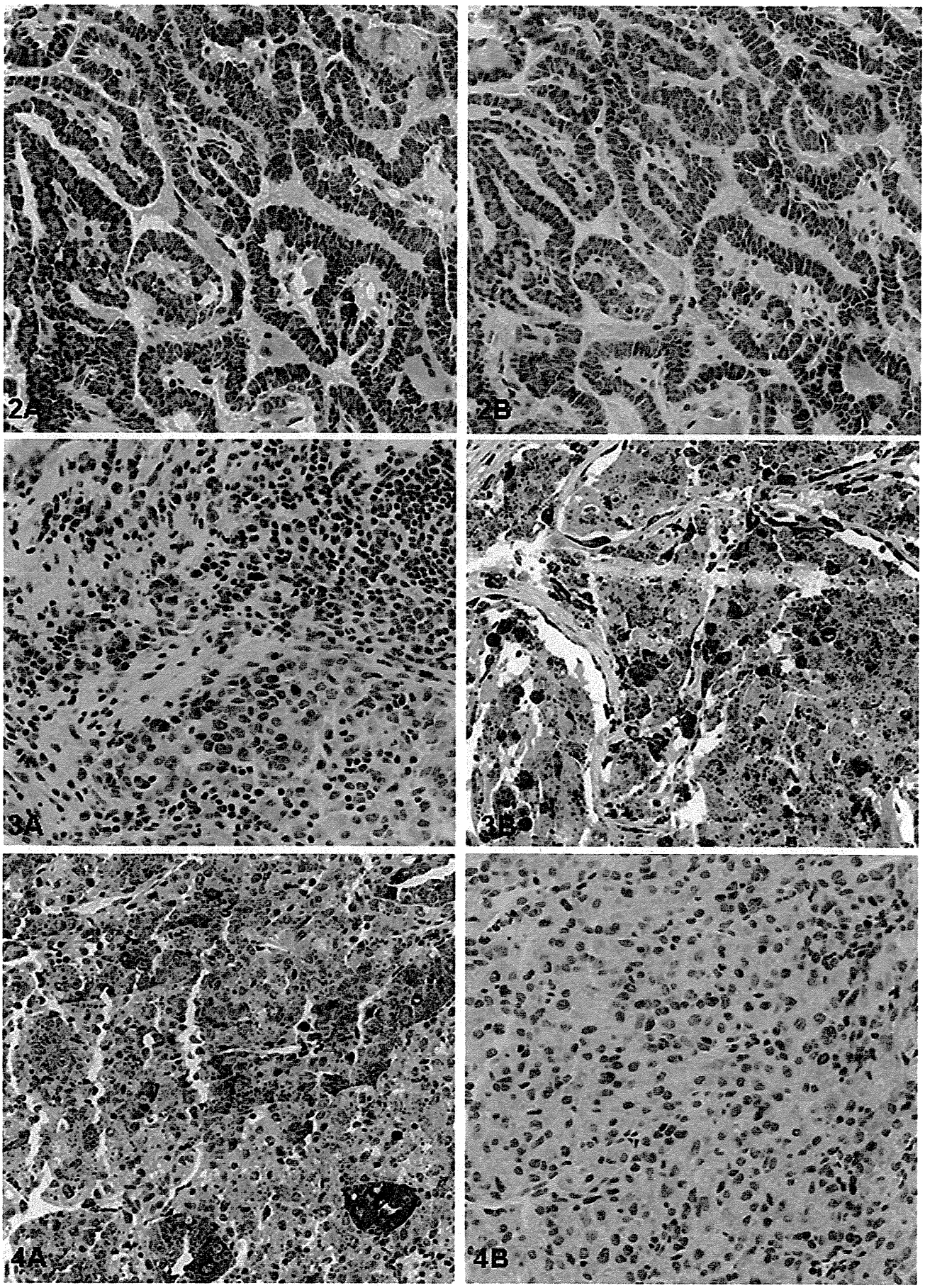
2A
2B
3A
3B
4A
4B

Table 5. Napsin A (Nap-A) Sensitivity, Specificity, Predictive Value (PV), and Likelihood Ratio (LR) for Primary Lung Adenocarcinoma Versus Primary Lung Small Cell Carcinoma

Stain Result	Lung Adenocarcinoma, No.	Small Cell Carcinoma, No.	Total	PV, % (PPV or NPV)	LR,[a] Result (PLR or NLR)
Nap-A$^+$	264	0	**264**	100 (PPV)	∞ (PLR)
Nap-A$^-$	39	52	**91**	52 (NPV)	0.13 (NLR)
Total	**303**	**52**	**355**		
	Sensitivity, 87%	Specificity, 100%			

Abbreviations: NLR, negative likelihood ratio; NPV, negative predictive value; PLR, positive likelihood ratio; PPV, positive predictive value; ∞, extremely high likelihood.

[a] Likelihood ratios may be better comparative indicators here than are predictive values (see "Statistical Methods" in text).

Table 6. Napsin A (Nap-A) and Thyroid Transcription Factor 1 (TTF-1) Sensitivity, Specificity, Predictive Value and Likelihood Ratio for Primary Lung Adenocarcinoma Versus Primary Lung Squamous Cell Carcinoma

Stain Result	Lung Adenocarcinoma, No.	Squamous Cell Carcinoma, No.	Total, No	PV, % (PPV or NPV)	LR,[a] Result (PLR or NLR)
Nap-A$^+$	264	5	**269**	98 (PPV)	34.85 (PLR)
Nap-A$^-$	39	195	**234**	83 (NPV)	0.13 (NLR)
Total	**303**	**200**	**503**		
	Sensitivity, 87%	Specificity, 98%			
TTF-1$^+$	60	2	**62**	97 (PPV)	30.00 (PLR)
TTF-1-	34	92	**126**	73 (NPV)	0.37 (NLR)
Total	**94**	**94**	**188**		
	Sensitivity, 64%	Specificity, 98%			

Abbreviations: LR, likelihood ratio; NLR, negative likelihood ratio; NPV, negative predictive value; PLR, positive likelihood ratio; PPV, positive predictive value; PV, predictive value.

[a] Likelihood ratios may be better comparative indicators here than are predictive values (see "Statistical Methods" in text).

Table 7. Napsin A (Nap-A) and Thyroid Transcription Factor 1 (TTF-1) Staining in Primary Lung Adenocarcinoma (PLA), Primary Lung Squamous Cell Carcinoma (PLSQ), and Primary Lung Small Cell Carcinoma (PLSC)

Tissue Type	Nap-A$^+$, TTF-1$^+$	Nap-A$^+$, TTF-1$^-$	Nap-A$^-$, TTF-1$^+$	Nap-A$^-$, TTF-1$^-$	Total
PLA	60	24	0	10	**94**
PLSQ	2	0	0	92	**94**
PLSC	0	0	48[a]	4[a]	**52**

[a] Primary lung small cell carcinoma tissues were not tested with TTF-1. The TTF-1 profile of primary lung small cell carcinoma was gleaned from the literature (90% of primary lung small cell carcinomas are positive for TTF-1).[19–27]

positive for Nap-A appears consistently to be the papillary type. This has been previously reported,[1,2] but, at this point, the numbers are too small to come to any meaningful conclusion. Again, we agree with Bishop and collegues[1] that, in the setting of a tumor positive for Nap-A with papillary architecture and "tall cell"–like features, immunohistochemistry for thyroglobulin should also be considered to exclude carcinoma of a thyroid origin. Additional studies may be helpful in clarifying this issue.

Having acknowledged the above, all of the nonpulmonary Nap-A–positive tumors stained weakly positive when compared against the negative control. In most cases the negative control actually showed minimal weak staining, making a positive result harder to interpret, and we may have actually *overestimated* the number of nonpulmonary tumors that showed positivity with Nap-A (Figures 1, A and B; 2, A and B; 4, A and B; and 5, A through D). The staining in the negative control may have been because of intrinsic biotin activity. In addition, the presence of macrophages and background should be considered when interpreting results. All the positive-staining pulmonary adenocarcinomas were strongly positive compared against a consistently negative (no staining) negative control. The Nap-A results were reported only after examining the tumor along with a negative control *of the same tumor specimen being evaluated.*

In summary, this study, the largest study of its kind to date, demonstrates that Nap-A is more sensitive and

←

Figure 2. *Napsin A. A, Positive staining in papillary thyroid carcinoma. B, Negative control, papillary thyroid carcinoma. Note the background staining in the negative control, which makes it a difficult-to-interpret "positive" result (original magnifications ×20 [A and B]).*

Figure 3. *Napsin A. A, Negative control, pulmonary squamous carcinoma. B, Positive staining in pulmonary squamous carcinoma. Note the weak-positive staining in the pulmonary squamous carcinoma. Compare that result to the strong-positive staining in the pulmonary adenocarcinoma (Figure 1, D). Both negative controls (Figures 1, C, and 3, A) in these 2 pulmonary lesions are "clean" (original magnifications ×20 [A and B]).*

Figure 4. *Napsin A. A, Positive staining in renal cell carcinoma. B, Negative control, renal cell carcinoma. Note the background staining in the negative control and the weak-positive staining in the tumor (original magnifications ×20 [A and B]).*

Table 8. Probable Lung Tumor Given Napsin A (Nap-A) and Thyroid Transcription Factor 1 (TTF-1) Staining in Primary Lung Adenocarcinoma (PLA), Primary Lung Squamous Cell Carcinoma (PLSQ), and Primary Lung Small Cell Carcinoma (PLSC)

Nap-A$^+$, TTF-1$^+$	Nap-A$^+$, TTF-1$^-$	Nap-A$^-$, TTF-1$^+$	Nap-A$^-$, TTF-1$^-$
PLA	PLA	PLSC	PLSQ

specific than TTF-1. Nap-A is better than TTF-1 in predicting the proportion of patients with positive test results (PPV, PLR) and negative test results (NPV, NLR) that are correctly diagnosed. Nap-A positivity is specific for primary lung adenocarcinoma when the major differential diagnosis includes primary small cell carcinoma. This is important because the surgical and chemotherapeutic options for these 2 tumors are markedly different. A combination of Nap-A and TTF-1 is useful in the distinction of primary lung adenocarcinoma from primary lung squamous cell carcinoma, and primary lung small cell carcinoma (primary lung adenocarcinoma, Nap-A$^+$/TTF-1$^\pm$; primary lung squamous cell carcinoma, Nap-A$^-$/TTF1$^-$; primary lung small cell carcinoma, Nap-A$^-$/TTF-1$^+$). Additional studies will be helpful in determining whether this is also true for less-poorly differentiated primary lung neuroendocrine tumors and small cell carcinomas of any origin. Consistent with previous studies and similar to most, if not all, immunohistochemical markers, Nap-A expression may be seen in other nonpulmonary tumors. The staining is generally weak and may actually be falsely positive when compared against a negative control of the same tumor specimen, whereas staining for primary lung adenocarcinoma is consistently, strongly positive, when compared against a negative control of the same tumor specimen. Consistent with previous studies, the tumors that are primarily implicated as challenging for the differential diagnosis include renal cell carcinoma and, possibly, papillary thyroid carcinoma.[1,2] If either of these 2 tumors, or for

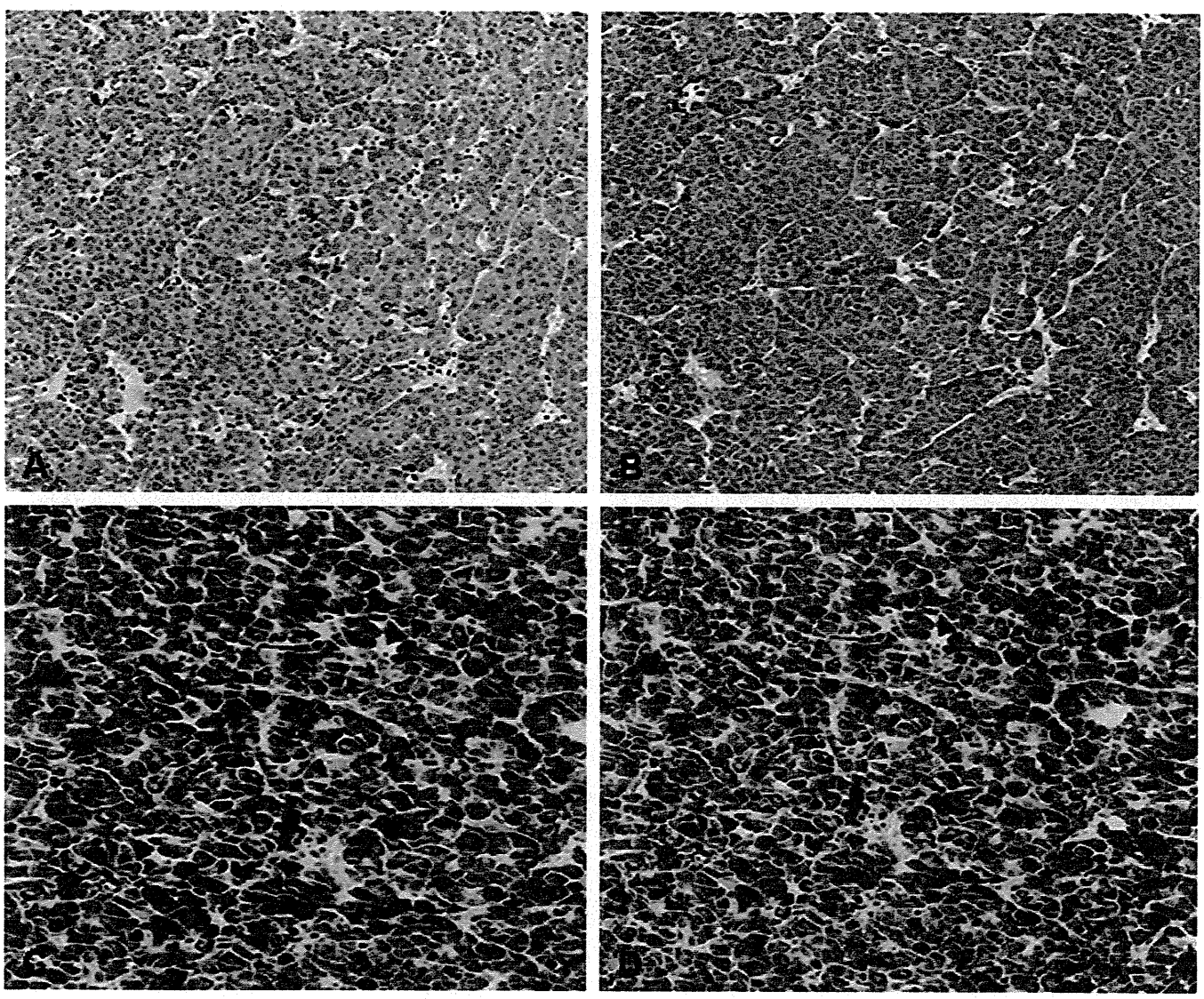

Figure 5. *Napsin A. A, Negative control, renal cell carcinoma. B, Positive staining in renal cell carcinoma. C, Negative control, renal cell carcinoma. D, Positive staining in renal cell carcinoma. In A, the background staining in the negative control makes it harder to interpret the "positive" result in B. Another marked example is seen in C and D. After much debate, D was called negative (original magnifications ×20 [A through D]).*

that matter, any of the other tumors evaluated in this study, are part of the differential diagnosis of primary lung adenocarcinoma, the addition of TTF-1 (negative in renal and other nonpulmonary, nonthyroid carcinomas), thyroglobulin (negative in lung adenocarcinoma, positive in papillary thyroid carcinoma), and other appropriate immunohistochemical markers, in addition to clinicoradiographic correlation, should help to distinguish the differences.

References

1. Bishop JA, Sharma R, Illei PB. Napsin A and thyroid transcription factor-1 expression in carcinomas of the lung, breast, pancreas, colon, kidney, thyroid, and malignant mesothelioma. *Hum Pathol.* 2010;41(1):20–25.
2. Ueno T, Linder S, Elmberger G. Aspartic proteinase napsin is a useful marker for diagnosis of primary lung adenocarcinoma. *Br J Cancer.* 2003;88(8):1229–1233.
3. Rosai, J. Respiratory tract: lung and pleura. In: Rosai J, ed. *Rosai and Ackerman's Surgical Pathology.* 9th ed. St. Louis, Missouri: Mosby Elsevier; 2004: 359–458.
4. Colby TV, Koss MN, Travis WD. Carcinoma of the lung: overview, incidence, etiology and screening. In: Rosai J, Sobin LH, eds. *Tumors of the Lower Respiratory Tract.* Washington, DC: Armed Forces Institute of Pathology; 1994:91–106. *Atlas Tumor of Pathology;* 3rd series, fascicle 13.
5. Loo PS, Thomas SC, Nicolson MC, Fyfe MN, Kerr KM. Subtyping of undifferentiated non–small cell carcinomas in bronchial biopsy specimens. *J Thorac Oncol.* 2010;5(4):442–447.
6. Rossi A, Maione P, Bareschino MA, et al. The emerging role of histology in the choice of first-line treatment of advanced non–small cell lung cancer: implication in the clinical decision-making. *Curr Med Chem.* 2010;17(11):1030–1038.
7. Cagle PT, Allen TC, Dacic S, et al. Revolution in lung cancer: new challenges for the surgical pathologist. *Arch Pathol Lab Med.* 2011;135(1):110–116.
8. Travis WD, Brambilla E, Noguchi M, et al. International Association for the Study of Lung Cancer/American Thoracic Society/European Respiratory Society International multidisciplinary lung adenocarcinoma classification. *J Thoracic Oncol.* 2011;6(2):244–285.
9. Cagle PT, Dacic S. Lung cancer and the future of pathology. *Arch Pathol Lab Med.* 2011;135(3):293–295.
10. Pavlides, N Briasoules, E, Hainsworth J, Greco FA. Diagnostic and therapeutic management of cancer of an unknown primary. *Eur J Cancer.* 2003; 39(14):1990–2005.
11. Varadhachary GR, Abbruzzese JL, Lenzi R. Diagnostic strategies for unknown primary cancer. *Cancer.* 2004;100(9):1776–1785.
12. Field RW, Smith BJ, Platz CE, et al. Lung cancer histologic type in the surveillance, epidemiology, and end results registry versus independent review. *J Natl Cancer Inst.* 2004;96(14):1005–1007.
13. Stang A, Pohlabeln H, Muller KM, Jahn I, Giersiepen K, Jockel KH. Diagnostic agreement in the histopathological evaluation of lung cancer tissue in a population-based case-control study. *Lung Cancer.* 2006;52(1):29–36.
14. Moreira A, Gonen M, Rekhtman N, Downey R. Progenitor stem cell marker expression by pulmonary carcinomas. *Mod Pathol.* 2010;23(6):889.895.
15. Jagirdar J. Application of immunohistochemistry to the diagnosis of primary and metastatic carcinoma of the lung. *Arch Pathol Lab Med.* 2008; 132(3):384–396.
16. Gu K, Shah V, Ma C, Zhang L, Yang M. Cytoplasmic immunoreactivity of thyroid transcription factor-1 (clone 8G7G3/1) in hepatocytes: true positivity or cross reaction? *Am J Clin Pathol.* 2007;128(3):382–388.
17. Lau SK, Luthringer DJ, Eisen RN. Thyroid transcription factor-1: a review. *Appl Immunohistochem Mol Morphol.* 2002;10(2):97–102.
18. Dejmek A, Naucler P, Smedjeback A, et al. Napsin A (TAO2) is a useful alternative to thyroid transcription factor-1 (TTF-1) for the identification of pulmonary adenocarcinoma of cells in pleural effusions. *Diagn Cytopathol.* 2007;35(8):493–497.
19. Dabbs D. Immunohistochemistry of metastatic carcinoma of unknown primary. In: Dabbs DJ, ed. *Diagnostic Immunohistochemistry.* 2nd ed. Philadelphia, Pennsylvania: Churchill Livingstone Elsevier; 2006:180–226.
20. DiLoreto C, Puglisi F, DiLauro V, Damante G, Fabbro D, Beltrami CA. Immunocytochemical expression of tissue specific transcription factor-1 in lung carcinoma. *J Clin Pathol.* 1997;50(1):30–32.
21. DiLoreto C, Puglisi F, DiLauro V, Damante G, Beltrami CA. TTF-1 protein expression in pleural malignant mesotheliomas and adenocarcinomas of the lung. *Cancer Lett.* 1998;124(1):73–78.
22. Fabbro D, DiLoreto C, Stamerra O, Beltrami CA, Lonigro R, Damante G. *TTF-1* gene expression and human lung tumors. *Eur J Cancer.* 1996;32A(3): 512–517.
23. Bejarno PA, Baughman RP, Biddinger PW, et al. Surfactant proteins and thyroid transcription factor 1 in pulmonary and breast carcinomas. *Mod Pathol.* 1996;9(4):445–452.
24. Lazzaro D, Price M, DeFelice M, DiLauro. The transcription factor TTF-1 is expressed at the onset of thyroid and lung morphogenesis and in restricted regions of the fetal brain. *Development.* 1991;113(4):1093–1104.
25. Stahlman MT, Gray ME, Whitsett JA. Expression of thyroid transcription factor-1 (TTF-1) and fetal and neonatal human lung. *J Histochem Cytochem.* 1996;44(7):673–678.
26. Fabbro D, DiLoreto C, Beltrami CA, Belfiore A, DiLauro R, Damante G. Expression of thyroid-specific transcription factors TTF-1 and PAX-8 in human thyroid neoplasms. *Cancer Res;* 54(17):4744–4749.
27. Katoh R, Kawaoi A, Miyagi E, et al. Thyroid transcription factor-1 in normal, hyperplastic, and neoplastic follicular thyroid cell examined by immunohistochemistry and nonradioactive in situ hybridization. *Mod Pathol;* 13(5):570–576.
28. Woischnik M, Bauer A, Aboutaam R, Pamir A, et al. Cathepsin H and napsin A are active in the alveoli and increased in alveolar proteinosis. *Eur Respir J.* 2008;31(6):1197–1204.
29. Yang M, Nonaka D. A study of immunohistochemical differential expression in pulmonary and mammary carcinomas. *Mod Pathol.* 2010;23(5): 654–661.
30. Brash F, Ochs M, Kahne T, et al. Involvement of napsin A in the C- and N-terminal processing of surfactant protein B in type-II pneumocytes of the human lung. *J Biol Chem.* 2003;278(49):49006–49014.
31. Suzuki A, Shijubo N, Yamada G, et al. Napsin A is useful to distinguish primary lung adenocarcinoma from adenocarcinoma from other organs. *Pathol Res Pract.* 2005;201(8–9):579–586.
32. Hirano T, Gong Y, Yoshida K, et al. Usefulness of TAO2 (napsin A) to distinguish primary lung adenocarcinoma from metastatic lung adenocarcinoma. *Lung Cancer.* 2003;41(2):155–162.
33. West RB, Harvell J, Linn SC, et al. Apo D in soft tissue tumors: a novel marker for dermatofibromasarcoma protuberans. *Am J Surg Pathol.* 2004;28(8), 1063–1069.
34. Deeks JJ, Altman DG. Diagnostic tests 4: likelihood ratios. BMJ. 2004; 329(7458):168–169.
35. Campbell SC, Novic AC, Bukowski RM. Renal tumors. In: Wein AJ, ed. *Campbell-Walsh Urology.* Vol 2. 9th ed. Philadelphia, Pennsylvania: Saunders Elsevier; 2007:1582–1632.